Computational Materials Science 210 (2022) 111419

Contents lists available at ScienceDirect

Computational Materials Science

journal homepage: www.elsevier.com/locate/commatsci

Full length article

Recent progress in the phase-field dislocation dynamics method

Shuozhi Xu

Department of Mechanical Engineering, University of California, Santa Barbara, CA 93106-5070, USA

ARTICLE INFO

Keywords:
Phase-field model
Dislocation dynamics
Crystalline materials

ABSTRACT

The phase-field dislocation dynamics (PFDD) method, originated in 2002, is a continuum dislocation model that uses order parameters to describe dislocation slips in crystalline materials. In the past two decades, and especially since it was last reviewed in 2016, PFDD was advanced significantly in terms of the mathematical formulation, numerical implementation, and applicability. The main purpose of this short review is to summarize recent progress made to improve the energy functional formulation and numerical techniques of PFDD as well as its recent applications. Some recommendations for future work to further extend the PFDD method are presented.

1. Introduction

Phase-field dislocation models are energy-based continuum dislocation models, in which dislocations are characterized by order parameters which evolve such that the free energy of the dislocated system approaches a local minimum [1]. The first phase-field dislocation model, termed phase-field microelasticity (PFM), was proposed by Khachaturyan and his colleagues [2] in 2001, taking advantage of the Khachaturyan–Shatalov microelasticity theory (KSMT). In the past two decades, different PFM variants were developed, differing in energy functional, initial and boundary conditions, and/or numerical techniques. Most variants kept the original name, e.g., the atomistic phase-field microelasticity (APFM) method developed by Mianroodi and Svendsen [3]. Other KSMT-based models, e.g., the microscopic phase-field (MPF) model developed by Shen et al. [4], do not contain "PFM" in their names.

One phase-field dislocation model that was influenced by PFM but did not take its name was developed by Koslowski et al. [5] in 2002. It was named the phase-field dislocation dynamics (PFDD) method for the first time in 2011 [6], and the name PFDD was used in most subsequent publications where this method was referred to. The PFDD method was last reviewed in 2016, by Beyerlein and Hunter [7]. Since then, PFDD has been significantly extended on multiple fronts. The purpose of this short review is to summarize recent developments and applications of PFDD, with a focus on those between 2016 and March 2022, and to provide the author's recommendations for future work to further advance this method for mechanics and materials science problems.

In general phase-field models, order parameters are employed to distinguish "phases", e.g., solid vs. liquid [8], face-centered cubic (FCC) crystal vs. body-centered cubic (BCC) crystal [9], and paramagnetic state vs. ferromagnetic state [10]. In phase-field dislocation models, each phase corresponds to a "state of slip", be it non-slipped, slipped by one dislocation, slipped by two dislocations, etc. Numerically, each phase is assigned an order parameter ϕ_α whose values are integers, e.g., 0, 1, 2, …, corresponding to the αth slip system. Individual dislocations are thus phase boundaries where at least one order parameter is not an integer. At a given continuum point $\boldsymbol{x}$, multiple phases, i.e., multiple states of slip, could co-exist. This suggests that the same point may be slipped by one dislocation within one slip system while unslipped within another system, in agreement with the physics of dislocation slip.

In its most general form to date, the total energy density ψ in PFDD contains four terms at $\boldsymbol{x}$: elastic energy density ψ_{ela}, lattice energy density ψ_{lat}, gradient energy density ψ_{gra}, and external energy density ψ_{ext}, i.e.,

$$\psi(\boldsymbol{x}) = \psi_{\text{ela}}(\boldsymbol{x}) + \psi_{\text{lat}}(\boldsymbol{x}) + \psi_{\text{gra}}(\boldsymbol{x}) - \psi_{\text{ext}}(\boldsymbol{x}). \tag{1}$$

Formulations of the four energy terms are motivated by the atomistic structure of a dislocation. An example is provided in Fig. 1, showing a dissociated edge dislocation in Cu based on a prior molecular static (MS) simulation [11]. ψ_{lat} represents the energy stored in atoms within the intrinsic stacking fault (ISF). ψ_{gra} represents the energy stored in atoms within the two Shockley partial dislocation cores. ψ_{ela} represents the energy stored in all atoms outside the ISF and partial cores. ψ_{ext} represents the energy arising from externally applied stress and/or strain.

Once the initial and boundary conditions are set, the time-dependent Ginzburg–Landau (TDGL) equation is used to update the order parameters such that the total energy (not its density) approaches a minimum, i.e.,

$$\dot{\phi}_\alpha(\boldsymbol{x}) = -m_0[\partial_{\phi_\alpha(\boldsymbol{x})}(\psi_{\text{ela}}(\boldsymbol{x}) + \psi_{\text{gsf}}(\boldsymbol{x}) - \psi_{\text{ext}}(\boldsymbol{x})) - \nabla \cdot \partial_{\nabla\phi_\alpha(\boldsymbol{x})}\psi_{\text{gra}}(\boldsymbol{x})] \tag{2}$$

E-mail address: shuozhixu@ucsb.edu.

https://doi.org/10.1016/j.commatsci.2022.111419
Received 8 March 2022; Received in revised form 30 March 2022; Accepted 31 March 2022
0927-0256/© 2022 Elsevier B.V. All rights reserved.

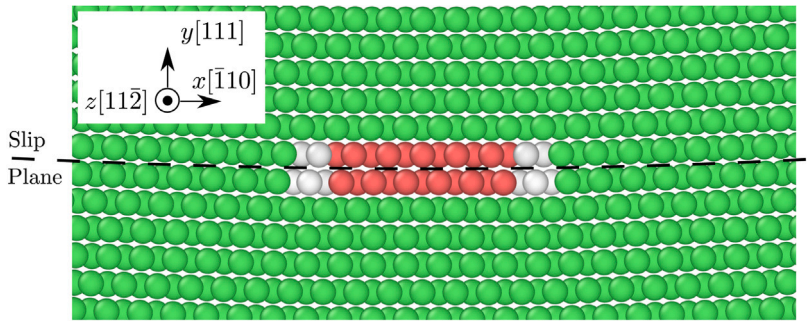

Fig. 1. An MS-based dissociated edge dislocation that belongs to a double tilt wall in a Cu thin film [11]. Visualization is realized in OVITO [12]. Based on the adaptive common neighbor analysis [13], red and white atoms correspond to those within the ISF and Shockley partial dislocation cores, respectively.

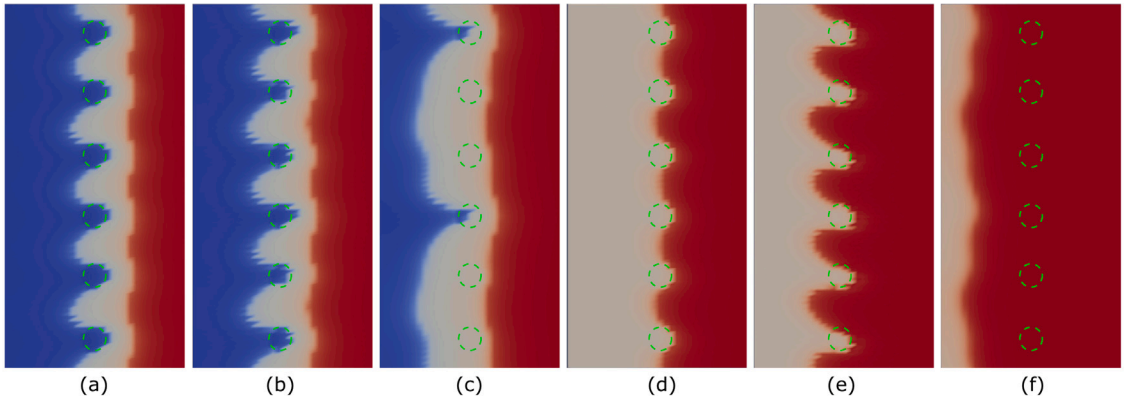

Fig. 2. Selected configurations for an edge dislocation bypassing six $Cu_{0.8}Nb_{0.2}$ precipitates in a Cu matrix. The applied stress is constant and is slightly higher than the critical stress. Snapshots are colored by the disregistry field ξ, where blue and red correspond to ξ being 0 and Burgers vector magnitude, respectively. Voids are denoted by dashed green circles.
Source: Reproduced with permission from Ref. [23].

where the superposed dot denotes the time derivative and the Ginzburg–Landau coefficient m_0 is non-negative.

In the remainder of this paper, recent advancements made to improve the four energy density terms and numerical techniques of PFDD as well as its recent applications will be reviewed.

2. Elastic energy

The original PFDD method assumed elastic isotropy in a homogeneous medium [5]. In 2019, Xu et al. [14] first implemented elastic anisotropy into PFDD, with details presented in a subsequent paper [15]. It was found that simplifying an elastically anisotropic medium to an isotropic one may result in incorrect predictions of the dislocation core structure [15–18], Peierls stress [17], non-Schmid effects [19], and dislocation transmission through an incoherent twin boundary (ITB) [20]. Thus, it is suggested that anisotropic elasticity always be used in PFDD simulations. Independent of the elastic anisotropy issue, elastic heterogeneity was introduced to PFDD to simulate a void in matrix in 2013 by Lei et al. [21] and a bi-phase material in 2016 by Zeng et al. [22]. Those two papers, however, assumed that the materials were elastic isotropic. The first time PFDD was applied to an elastically anisotropic, bi-phase medium was in 2022, when Xu et al. [23] studied dislocation/obstacle interactions, as shown in Fig. 2. Note that the elastic heterogeneity is realized in PFDD following Eshelby's inclusion theory [24] which requires introduction of an order parameter-like quantity: virtual strain tensor. As a result, the elastic energy density formulation is revised and an additional set of TDGL is needed to minimize the total energy of the system with respect to each component of the virtual strain tensor.

Outlook: All PFDD work to date addressed either single-phase or bi-phase materials. In the meantime, most real-world materials contain multiple phases that vastly differ in their size, from micron to nanoscale, and in properties, such as elasticity and crystal structure. To simulate dislocation dynamics in these multi-phase materials, the elastic energy in PFDD should be further extended. Such an extension has been achieved in PFM to model dislocation dynamics in a system containing a thin film, a substrate, and a vacuum [25].

3. Lattice energy

In the original PFDD method, the lattice energy density was a piecewise quadratic function of the order parameter [5]. The idea was that the lattice energy should mimic the Peierls potential, i.e., the energy pathway along which the dislocation moves between two Peierls valleys. Only one slip system was considered per slip plane. In 2004, Koslowski and Ortiz [26] extended PFDD to three slip systems per slip plane. However, for each dislocation, only one slip system, represented by one order parameter, was considered. Then in 2011, Lei and Koslowski [6] used the generalized stacking fault energy (GSFE) curve to approximate the Peierls potential, and a $\sin^2$ function was used to approximate the GSFE. Since there was no local minimum, both quadratic and sinusoidal functions resulted in undissociated dislocations. Later that year, Lee et al. [27] used a fourth-order polynomial for an undissociated dislocation and a six-order polynomial (which contains a local minimum) for a dissociated one. In all four papers, only one order parameter was adopted for each dislocation. On the other hand, three of those papers [5,26,27] studied FCC crystals, in which three slip systems co-exist to describe a dissociated dislocation.

To better link physics and the PFDD model for FCC metals, Hunter et al. [28] used a Fourier series function to construct the GSFE surface in 2011. The function has seven unknown parameters which are obtained from atomistic simulations. Three order parameters, each

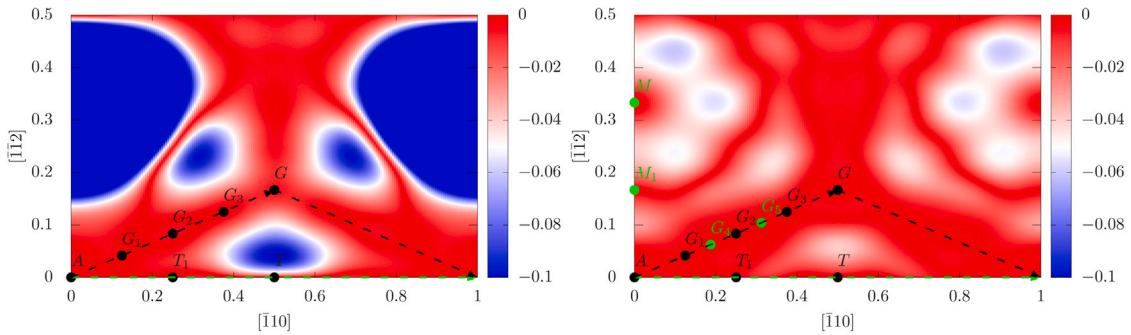

(a) Seven-term (b) Eleven-term

Fig. 3. The difference between the GSFE surface based on (a) a seven-term Fourier series function or (b) an eleven-term Fourier series function and the actual GSFE surface on the (111) plane in Au. GSFEs are in units of J/m^2. The seven or eleven points selected to fit the Fourier series functions are highlighted.
Source: Adapted with permission from Ref. [16].

of which corresponds to a ⟨110⟩{111} slip system, were used per dislocation. Since the ⟨110⟩{111} slip vector would dissociate into two non-parallel ⟨112⟩{111} vectors on the GSFE surface upon energy minimization, those PFDD simulations naturally yielded dissociated dislocations. Later, in 2014, Hunter et al. [29] used density functional theory (DFT) calculation data to inform the seven-term Fourier series function. In 2019, an eleven-term Fourier series function, developed by Xu et al. [16], was shown to better approximate the actual GSFE surface than the seven-term one (Fig. 3). In the same paper, the authors developed a PFDD model in which the GSFE surface was constructed using discrete data from atomistic simulations instead of from a continuous function. Later, Xu et al. [15] conducted PFDD simulations using GSFE surfaces that are directly from DFT calculations of Su et al. [30].

In BCC crystals, slip vectors are along ⟨111⟩ directions on three possible slip plane groups: {110}, {112}, and {123}. Unlike its counterpart in FCC crystals, a slip vector in BCC crystals does not dissociate upon energy minimization on either of the three GSFE surfaces [31]. Therefore, only one order parameter is used per slip plane, and the lattice energy is then related to a GSFE curve, instead of a surface. Since there is no local minimum along this curve, the PFDD-predicted dislocation is undissociated, in agreement with atomistic simulations. Like the GSFE surface, the GSFE curve may be either approximated using a continuous function (e.g., a one-term $\sin^2$ function) [32–34] or directly calculated from atomistic or DFT calculations [35]. PFDD simulations using a one-term $\sin^2$ function predicted higher critical stresses for the Frank–Read source operation in two BCC metals than those using GSFE curves made of discrete DFT data [35]. Indeed, it was shown in the same paper that a two-term $\sin^2$ function provided a better approximation of the GSFE curve than the one-term one.

Recall that the GSFE curve was initially proposed to approximate the Peierls potential [6], which differs greatly among dislocations with different character angles in BCC metals [36]. To account for such anisotropy, the GSFE, which is character angle-independent, may be multiplied by an angle-dependent scaling factor [32]. It was shown that such a modification resulted in a better prediction of the dislocation loop shape [33]. Alternatively, the GSFE scaling factor may be a function of the applied shear stress and the angle between the maximum resolved shear stress plane (MRSSP) and the glide plane, as one way to capture the non-Schmid effects in BCC metals [19]. Another way to model the non-Schmid effects is through adjusting the gradient energy coefficients, which will be discussed in Section 4.

In hexagonal close-packed (HCP) crystals, possible slip planes include basal, prismatic-I, pyramidal-I, and pyramidal-II planes [37]. To date, PFDD simulations have been applied to studying ⟨a⟩ dislocation on the basal plane, ⟨a⟩ dislocation on the prismatic-I plane, and ⟨$a+c$⟩ dislocation on the pyramidal-II plane [18,38]. Since the basal plane in HCP crystals is similar to the {111} plane in FCC crystals, a seven-term Fourier series function was used to approximate the GSFE surface [38]. Three order parameters were used per basal plane, and the dislocation was dissociated upon energy minimization. Within the pyramidal-II GSFE surface, the ⟨$a+c$⟩ slip vector dissociates to two co-linear smaller vectors upon energy minimization in ten HCP metals [18]. The prismatic-I plane is more complicated. First, it is corrugated, i.e., there exist closely- and loosely-spaced planes [39]; PFDD was applied to only the loosely-spaced prismatic-I planes on which the dislocation glide is easier [40]. Second, the slip vector within the loosely-spaced prismatic-I plane dissociates to two co-linear vectors in Ti and Zr but undissociates in Mg [38]. Thus, only a GSFE curve is needed per prismatic-I or pyramidal-II plane. In Refs. [18,38], each GSFE curve was approximated by a DFT-informed nine-term Fourier series function, although they could have been based on direct DFT calculations. Overall, in HPC crystals, the PFDD-based dislocations are dissociated in most cases.

Another line of advancing the lattice energy is to make it spatially variable. This feature is needed in modeling multi-principal element alloys in which the GSFE depends on the atomic-scale local chemical composition [41]. In 2019, Zeng et al. [42] and Su et al. [43] used PFDD to model dislocations in FCC MPEAs. More recently, Smith et al. [33] and Fey et al. [34] explored dislocation dynamics in a BCC MPEA using PFDD. Examples of dislocation glide in MPEAs are shown in Fig. 4. It is worth mentioning that the spatial variation in lattice energy usually requires a large number of PFDD simulations, which naturally result in a large amount of data. Rather than attempting to relate the inputs and outputs analytically, the task is better done via machine learning (ML). Indeed, the PFDD data from Zeng et al. [42] have been processed using ML by Vilalta et al. [44].

Taken together, it is suggested that (i) DFT data are preferable to atomistic simulation data and (ii) direct atomic-level calculation-based GSFE surfaces or curves are preferable to those based on continuous functions. Note that in a heterogeneous material, the lattice energy is non-zero only in phase(s) where dislocations exist.

Outlook: To date, the PFDD model has not been applied to slips on the pyramidal-I plane in HCP crystals, although doing so would be straightforward. Like the prismatic-I plane, the pyramidal-I plane is also corrugated, and so there are loosely- and densely-closed planes [39]. There are two types of slip vectors, ⟨a⟩ and ⟨$a+c$⟩, within each type of pyramidal-I plane. From the GSFE surfaces on the loosely-spaced pyramidal-I planes in Mg, Ti, and Zr [40], one sees that, upon energy minimization, the ⟨$a+c$⟩ vector would dissociate into two non-parallel ones, while the ⟨a⟩ vector would not dissociate. On the densely-spaced pyramidal-I planes in Ti and Zr, it is the opposite: the ⟨a⟩ vector dissociates into two non-parallel ones, while the ⟨$a+c$⟩ vector does not dissociate [40].

In any crystal structures, the rule of thumb is that a GSFE surface should be used in PFDD if the slip vector dissociates to two or more vectors and at least one of them is not parallel to the original vector;

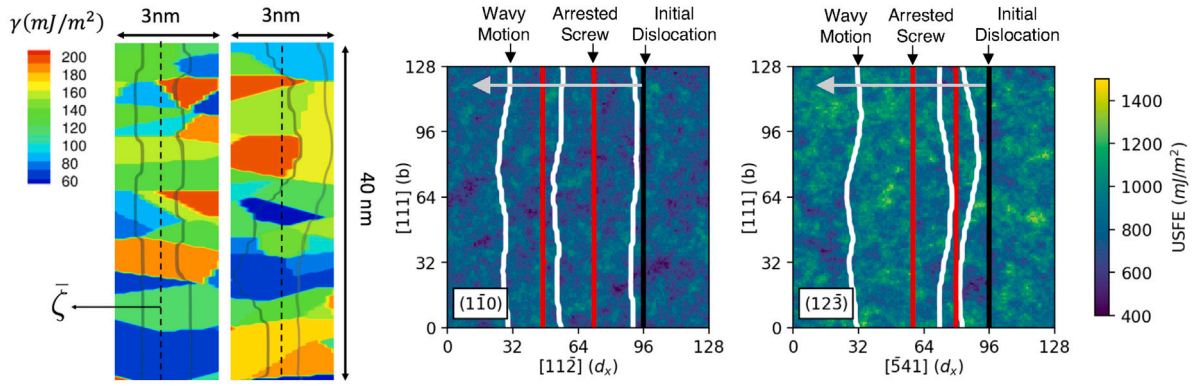

(a) FCC CoCrFeMnNi (b) BCC MoNbTi

Fig. 4. (a) Gliding of a dissociated edge dislocation in an FCC CoCrFeMnNi MPEA. Different ISF energies are assigned randomly to different regions within a {111} slip plane. (b) Gliding of an undissociated screw dislocation in a BCC MoNbTi MPEA within a {110} or a {123} slip plane. The background is colored by local unstable stacking fault energy (USFE). The initially straight dislocation (in black) becomes wavy during glide (in white) under stress but is then arrested and returns to a straight morphology (in red). *Source:* (a) is reproduced with permission from Ref. [42]. (b) is reproduced with permission from Ref. [34].

a GSFE curve should be employed if the slip vector dissociates to two or more vectors that are all parallel to the original one, or it does not dissociate at all. Should the GSFE surface be used, the PFDD-predicted dislocation would be dissociated; should the GSFE curve be employed, the dislocation would be dissociated if at least one local minimum exists on the curve; otherwise, the dislocation would not be dissociated.

4. Gradient energy

The original PFDD model did not include the gradient energy term in its total energy [5]. That PFDD version was shown to be physically equivalent to the generalized Peierls–Nabarro model [45]. In 2019, the gradient energy was added to the PFDD model by Xu et al. [14]. The augmented model has been compared against the original one to assess the effects of the gradient energy on the dislocation core structure [14,15,17,43], Peierls stress [17], and non-Schmid effects [19]. In most cases, the gradient energy leads to a more diffuse core configuration and a lower Peierls stress. Including the gradient energy is generally desirable in FCC metals because it results in a core structure in better agreement with atomistic simulations, as shown in Fig. 5(a); yet there are some exceptions [15].

If it has been decided that the gradient energy should be included in a PFDD simulation, the next step is to determine the gradient energy coefficients. Although there are two independent coefficients, most PFDD simulations to date assumed that they have the same value. It was shown that non-uniform coefficients are better than the uniform one because the former predicts a better dislocation core structure [17]. Therefore, it is suggested that non-uniform coefficients be used whenever possible. On the other hand, regardless of whether the gradient energy coefficients are uniform or not, there are three ways to determine their values in PFDD. Each way adjusts the coefficients such that the corresponding PFDD simulation results, being either ISF width [15,17,43], core width [19], or disregistry field [14], agree well with atomistic simulation data. Note that Kim et al. [19] tailored the gradient energy coefficients such that the core width would correctly yield the non-Schmid effects, as shown in Fig. 5(b). Like the lattice energy, the gradient energy in a heterogeneous material is non-zero only in phase(s) where dislocations exist.

Outlook: To date, the gradient energy coefficients were determined by fitting PFDD-derived core structures to those of atomistics, even when the GSFEs were DFT-based [15,43]. That was because it was much easier to model a dislocation using atomistic simulations than DFT. Future work may fit the gradient energy coefficients to DFT-based dislocation core structures, especially when modeling materials whose GSFEs are from DFT.

5. External energy

The original PFDD model only allowed for stress-controlled loading [5]. In 2015, the strain-controlled loading feature was added to PFDD by Cao et al. [46]. Recently, Kim et al. [19] modified the stress-based external energy to account for the inclined and perpendicular stress components, but the corresponding PFDD simulations did not correctly reproduce the non-Schmid effects (see the golden curve in Fig. 5(b)). Note that in a heterogeneous material, one needs to slightly revise the external energy density formulation to involve the virtual strain tensor [23].

6. Numerical techniques

The original PFDD model required no computational grid [5]. In 2004, Koslowski and Ortiz [26] introduced 2D numerical grids to PFDD simulations to describe a dislocation network. Then in 2011, 3D grids were used for the first time [6]. In that application, the undeformed simulation cell contained a few dislocations within one slip plane; then during loading, new dislocations on other slip planes were nucleated in the absence of sources on those planes. However, it is difficult to ensure the accuracy of the critical stress for homogeneous dislocation nucleation in either phase-field dislocation model [47] or Peierls–Nabarro model [48]. On the other hand, the theoretical framework of the phase-field dislocation model, e.g., PFM [2], assumes that for one dislocation, its inelastic displacement field is confined to the slip plane. Taking this point into consideration and following the MPF model [4], Xu et al. [14] developed a PFDD model that confined all slips to pre-defined slip planes. That PFDD model was shown to result in a more diffuse dislocation core and a lower Peierls stress than the non-confined version. If only one slip plane is activated, imposing this confinement would reduce the problem to 2D. However, problems involving multiple active slip planes (e.g., Refs. [49,50]) remain 3D even when the confinement is applied. In either 2D or 3D problems, the confinement precludes most, if not all, homogeneous dislocation nucleation.

All numerical grids discussed above were orthogonal. In 2021, Peng et al. [51] developed non-orthogonal 3D numerical grids for FCC and BCC metals. One advantage of this type of grids is that it reduces the Gibbs oscillations (caused by the fast Fourier transform (FFT) algorithm) and better describes dislocation annihilation (Fig. 6(a)), compared with the orthogonal grids. Another advantage is that non-orthogonal grids can capture the process of screw dislocation cross-slip [52], as shown in Fig. 6(b). Note that since cross-slip concerns

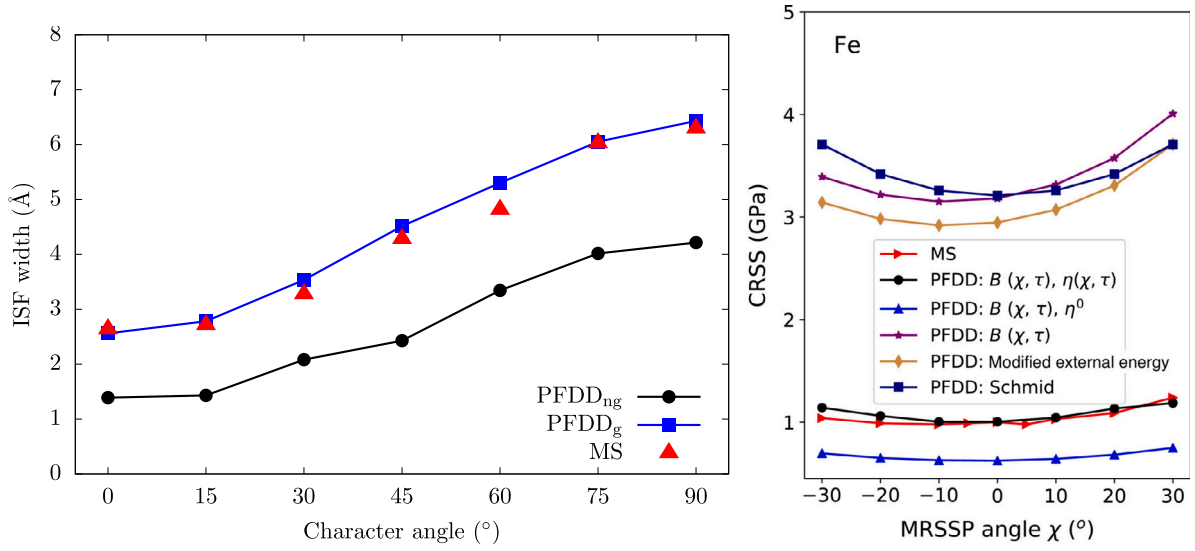

(a) FCC Al (b) BCC Fe

Fig. 5. (a) ISF widths of seven dislocations with different character angles in FCC Al, predicted by PFDD and MS simulations. PFDD$_g$ and PFDD$_{ng}$ refer to PFDD models with and without the gradient energy term, respectively. (b) The critical resolved shear stress (CRSS) of a screw dislocation in BCC Fe, predicted by different PFDD models, MS, and Schmid law. B, η, τ, and χ are GSFE scaling factor, uniform gradient energy coefficient, applied shear stress, and the angle between the MRSSP and the glide plane, respectively.
Source: (a) is adapted with permission from Ref. [14]. (b) is adapted with permission from Ref. [19].

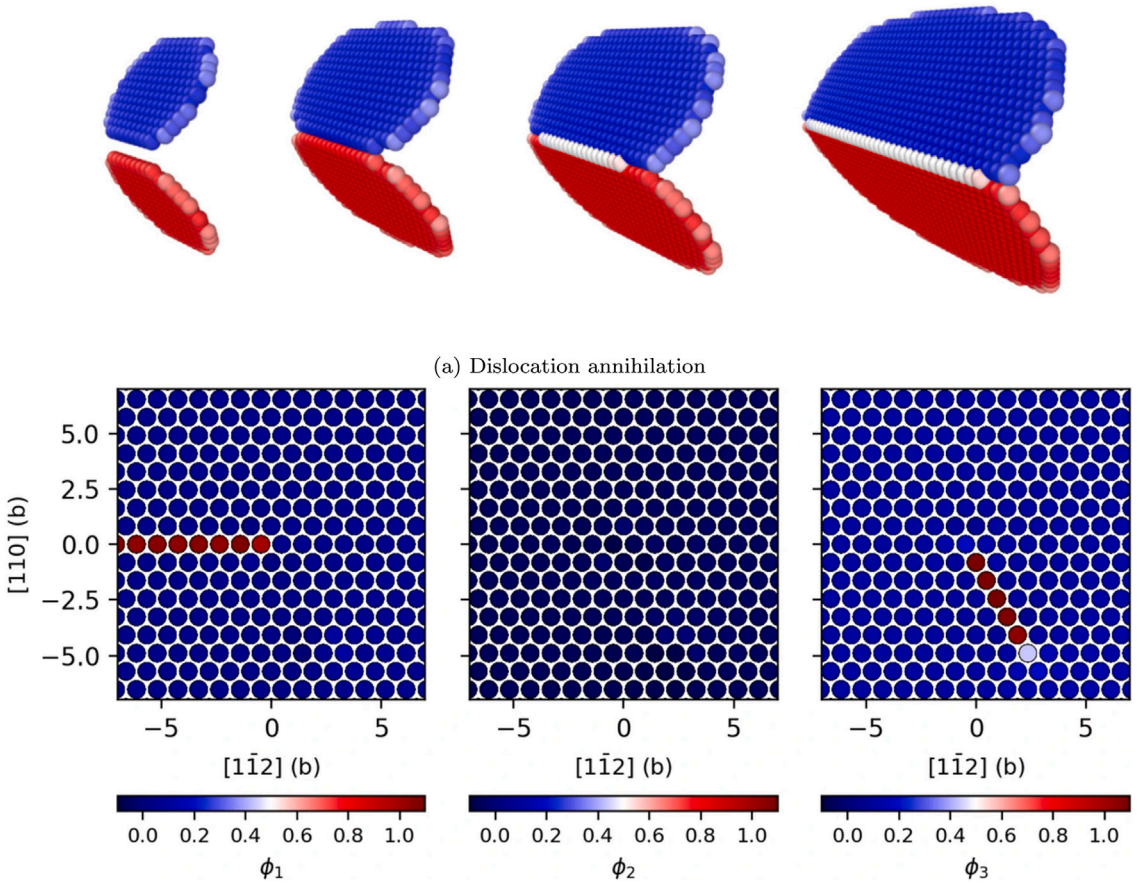

(a) Dislocation annihilation

(b) Dislocation cross-slip

Fig. 6. (a) Snapshots of two dislocation loops expanding in a 3D non-orthogonal grid. The loops expand, meet, and annihilate at the screw segment marked in white. (b) Cross-slip of a screw dislocation from the (110) plane to the (101) plane. ϕ_1, ϕ_2, and ϕ_3 are three order parameters.
Source: (a) is adapted with permission from Ref. [51]. (b) is reproduced with permission from Ref. [52].

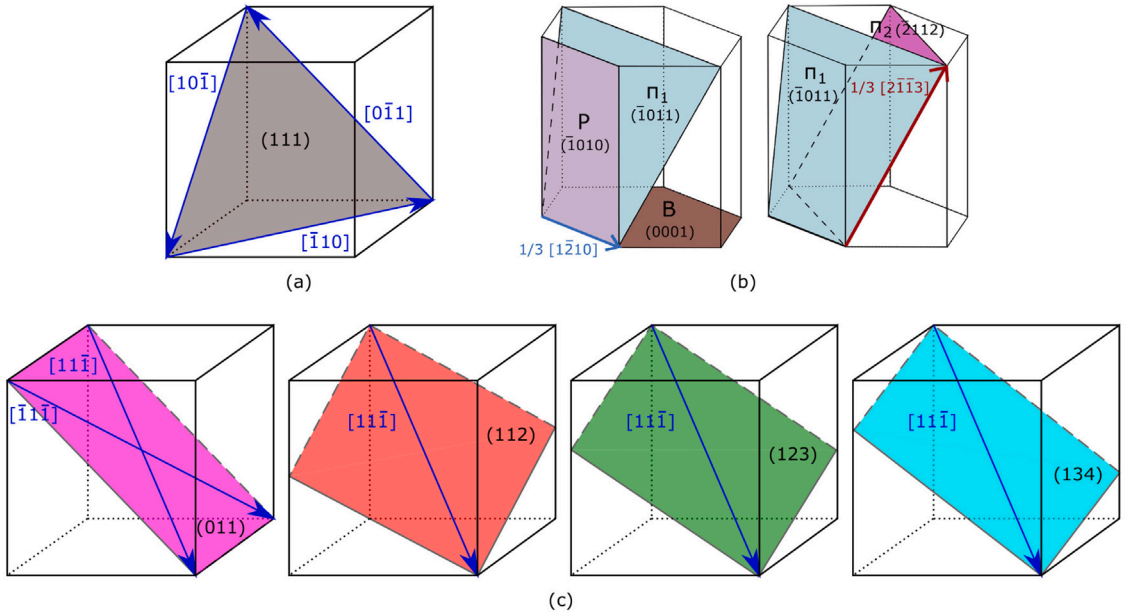

Fig. 7. (a) FCC structure showing a {111} slip plane with three ⟨110⟩ dislocations. (b) HCP structure showing four slip planes with ⟨a⟩ and ⟨$c + a$⟩ dislocations. B: basal plane; P: prismatic-I plane; π: pyramidal plane. (c) BCC structure showing four slip planes with ⟨111⟩ dislocations. In all subfigures, Burgers vectors are denoted as arrows.
Source: (b) is reproduced with permission from Ref. [40].

a change of slip plane for the same dislocation, the aforementioned slip confinement should not be imposed.

Over the years, efforts were also made to accelerate the PFDD code. In 2011, the code was parallelized via message passing interface [53]. Then in 2018, it was alternatively sped up by graphics processing unit [54].

Outlook: The spacings in 3D orthogonal grids were studied by Xu et al. in both FCC [17] and BCC metals [35]. It was found that grid spacings with atomic resolution should be applied if PFDD-based disregistry fields were to match those from atomistic simulations. However, since the grid was uniform, a fine grid spacing is used even in regions far from the dislocation cores. One way to improve the computational efficiency is to employ non-uniform grids which are adaptively refined near dislocation cores. This has been achieved in a GPN model [55], and should be implementable in PFDD as long as the current FFT algorithm is properly revised to handle non-uniform grids [56].

Another issue in PFDD is that currently periodic boundary conditions must be applied on all three directions of the simulation cell. This is a requirement of the FFT algorithm that is used to solve the elastic energy. If the finite element method (FEM) were used instead, more flexible boundary conditions could be considered. A comparison between FFT and FEM in crystal plasticity simulations has been presented by Liu et al. [57], shedding light on how the current PFDD code could be revised.

7. Applications

7.1. Crystal structure

As discussed in Section 3, the original PFDD method was for {111} planes in FCC crystals [5]. In 2020, Peng et al. [32] extended PFDD to slips on {110} planes in BCC metals. Later that year, Xu et al. [35] further extended it to {112} and {123} slip planes in BCC metals. Then in 2022, Fey et al. [34] studied slips on {134} planes in a BCC MPEA. Alternative to cubic crystals, Albrecht et al. [38] carried out PFDD simulations in 2020 to model dislocations on basal, prismatic-I, and pyramidal-II planes in HCP metals. Common slip systems in FCC, BCC, and HCP crystals are illustrated in Fig. 7.

Outlook: The PFDD model is applicable to slips on any crystallographic plane in any crystal. Thus, there is no theoretical challenge in applying PFDD to more crystal structures. In PFDD simulations to date, a material, even the bi-phase one [22,23], had a uniform crystal structure. Future PFDD work may consider a bi-phase or multi-phase material in which two or more crystal structures co-exist.

7.2. Mechanics and materials science problems

The original PFDD model studied slips on a single plane [5]. In 2014, Hunter and Beyerlein [49] used PFDD to simulate slips on two pre-defined, parallel slip planes. Only after the non-orthogonal grids were developed in 2021 [51] was PFDD applied to slips on non-parallel planes such as dislocation annihilation [51] and cross-slip [52]. However, the lattice energy formulation needs to be further revised if PFDD were to study more complex dislocation intersections such as lock formation. This has been achieved in PFM, although only undissociated dislocations were considered [58].

The original PFDD model studied slips in a single crystal [5]. In 2015, Cao et al. [46] extended PFDD to nano-crystals, while assuming isotropic elasticity. In 2022, Ma et al. [20] used PFDD to study a bi-crystal containing an ITB. They compared results based on isotropic and anisotropic elasticity. However, since the ITB is a special boundary, the elastic tensors in both grains were the same, and so the bi-crystal was effectively elastically homogeneous. To account for elastic anisotropy in more general bi- or nano-crystals, virtual strain tensor [22,23] should be introduced.

The original PFDD model studied slips in a pure metal [5]. In 2019, Zeng et al. [42] extended PFDD to MPEAs, by spatially varying the lattice energy, as discussed in Section 3.

In current PFDD model, the total energy density contains four terms (Eq. (1)). Some other phase-field dislocation models, however, add chemical potential to the total energy [59–61] to simulate interactions between dislocations and solutes or crystalline precipitates. In those models, a new set of order parameters, representing the chemical concentration of solutes, was introduced. Since the solute concentration was conservative, the Cahn–Hilliard diffusion equation, instead of the TDGL (Eq. (2)), was used to update the new order parameters. These

features can be included into PFDD to explore dislocation dynamics in the presence of solutes such as hydrogen and oxygen.

In addition to solutes and crystalline precipitates, more complex defects such as twins, amorphous precipitates, and general grain boundaries may also be considered in future PFDD work with the help of the virtual strain tensor. In particular, current PFDD model assumes that amorphous materials are unshearable by dislocations and do not undergo any plasticity. However, it is known that amorphous materials can deform plastically via, e.g., shear transformation zone [62]. An additional set of order parameters may to be introduced to characterize the plastic deformation of amorphous materials.

Lastly, most, if not all, PFDD simulations to date are deterministic. Recent discrete dislocation dynamic simulations showed that important phenomena such as dislocation wall formation is reproduced only when the dislocation dynamics becomes stochastic, enabled by the Monte Carlo method [63]. On the other hand, stochastic phase-field method has been applied to brittle fracture [64], but not to any dislocation model. It will be useful to develop stochastic PFDD method in the future.

8. Conclusions

In this paper, developments and applications of the PFDD method in the past two decades are reviewed, with a focus on those since 2016 when PFDD was last reviewed [7]. Advancements made to improve the four energy density terms and numerical techniques are individually discussed, followed by a brief summary of applications of PFDD to date. Some recommendations for future work to further extend the PFDD method are presented throughout the paper.

Declaration of competing interest

The author declares that he has no known competing financial interests or personal relationships that could have appeared to influence the work reported in this paper.

Acknowledgment

The author is supported by the Department of Energy, Office of Science, Basic Energy Sciences Program, USA DE-SC0020133.

References

[1] Y. Wang, J. Li, Phase field modeling of defects and deformation, Acta Mater. 58 (4) (2010) 1212–1235, http://dx.doi.org/10.1016/j.actamat.2009.10.041.
[2] Y.U. Wang, Y.M. Jin, A.M. Cuitiño, A.G. Khachaturyan, Nanoscale phase field microelasticity theory of dislocations: model and 3D simulations, Acta Mater. 49 (10) (2001) 1847–1857, http://dx.doi.org/10.1016/S1359-6454(01)00075-1.
[3] J.R. Mianroodi, B. Svendsen, Atomistically determined phase-field modeling of dislocation dissociation, stacking fault formation, dislocation slip, and reactions in fcc systems, J. Mech. Phys. Solids 77 (2015) 109–122, http://dx.doi.org/10.1016/j.jmps.2015.01.007.
[4] C. Shen, J. Li, Y. Wang, Predicting structure and energy of dislocations and grain boundaries, Acta Mater. 74 (2014) 125–131, http://dx.doi.org/10.1016/j.actamat.2014.03.065.
[5] M. Koslowski, A.M. Cuitiño, M. Ortiz, A phase-field theory of dislocation dynamics, strain hardening and hysteresis in ductile single crystals, J. Mech. Phys. Solids 50 (12) (2002) 2597–2635, http://dx.doi.org/10.1016/S0022-5096(02)00037-6.
[6] L. Lei, M. Koslowski, Mesoscale modeling of dislocations in molecular crystals, Phil. Mag. 91 (6) (2011) 865–878, http://dx.doi.org/10.1080/14786435.2010.533135.
[7] I.J. Beyerlein, A. Hunter, Understanding dislocation mechanics at the mesoscale using phase field dislocation dynamics, Philos. Trans. R. Soc. A 374 (2066) (2016) 20150166, http://dx.doi.org/10.1098/rsta.2015.0166.
[8] W.J. Boettinger, J.A. Warren, C. Beckermann, A. Karma, Phase-field simulation of solidification, Annu. Rev. Mater. Res. 32 (1) (2002) 163–194, http://dx.doi.org/10.1146/annurev.matsci.32.101901.155803.
[9] M. Mamivand, M.A. Zaeem, H. El Kadiri, A review on phase field modeling of martensitic phase transformation, Comput. Mater. Sci. 77 (2013) 304–311, http://dx.doi.org/10.1016/j.commatsci.2013.04.059.
[10] T. Koyama, Phase-field modeling of microstructure evolutions in magnetic materials, Sci. Tech. Adv. Mater. 9 (1) (2008) 013006, http://dx.doi.org/10.1088/1468-6996/9/1/013006.
[11] J. Xu, S. Xu, I.J. Beyerlein, Atomistic simulations of dipole tilt wall stability in thin films, Thin Solid Films 689 (2019) 137457, http://dx.doi.org/10.1016/j.tsf.2019.137457.
[12] A. Stukowski, Visualization and analysis of atomistic simulation data with OVITO — the open visualization tool, Modelling Simul. Mater. Sci. Eng. 18 (1) (2010) 015012, http://dx.doi.org/10.1088/0965-0393/18/1/015012.
[13] A. Stukowski, Structure identification methods for atomistic simulations of crystalline materials, Modelling Simul. Mater. Sci. Eng. 20 (4) (2012) 045021, http://dx.doi.org/10.1088/0965-0393/20/4/045021.
[14] S. Xu, L. Smith, J.R. Mianroodi, A. Hunter, B. Svendsen, I.J. Beyerlein, A comparison of different continuum approaches in modeling mixed-type dislocations in Al, Modelling Simul. Mater. Sci. Eng. 27 (7) (2019) 074004, http://dx.doi.org/10.1088/1361-651X/ab2d16.
[15] S. Xu, Y. Su, I.J. Beyerlein, Modeling dislocations with arbitrary character angle in face-centered cubic transition metals using the phase-field dislocation dynamics method with full anisotropic elasticity, Mech. Mater. 139 (2019) 103200, http://dx.doi.org/10.1016/j.mechmat.2019.103200.
[16] S. Xu, J.R. Mianroodi, A. Hunter, I.J. Beyerlein, B. Svendsen, Phase-field-based calculations of the disregistry fields of static extended dislocations in FCC metals, Phil. Mag. 99 (11) (2019) 1400–1428, http://dx.doi.org/10.1080/14786435.2019.1582850.
[17] S. Xu, J.R. Mianroodi, A. Hunter, B. Svendsen, I.J. Beyerlein, Comparative modeling of the disregistry and Peierls stress for dissociated edge and screw dislocations in Al, Int. J. Plast. (2020) 102689, http://dx.doi.org/10.1016/j.ijplas.2020.102689.
[18] C. Albrecht, A. Kumar, S. Xu, A. Hunter, I.J. Beyerlein, Asymmetric equilibrium core structures of pyramidal II $\langle c+a \rangle$ dislocations in ten hexagonal close packed metals, Phys. Rev. Mater. 5 (2021) 043602, http://dx.doi.org/10.1103/PhysRevMaterials.5.043602.
[19] H. Kim, N. Mathew, D.J. Luscher, A. Hunter, Phase field dislocation dynamics (PFDD) modeling of non-Schmid behavior in BCC metals informed by atomistic simulations, J. Mech. Phys. Solids 152 (2021) 104460, http://dx.doi.org/10.1016/j.jmps.2021.104460.
[20] T. Ma, H. Kim, N. Mathew, D.J. Luscher, L. Cao, A. Hunter, Dislocation transmission across $\Sigma 3\{112\}$ incoherent twin boundary: a combined atomistic and phase-field study, Acta Mater. 223 (2022) 117447, http://dx.doi.org/10.1016/j.actamat.2021.117447.
[21] L. Lei, J.L. Marin, M. Koslowski, Phase-field modeling of defect nucleation and propagation in domains with material inhomogeneities, Modelling Simul. Mater. Sci. Eng. 21 (2) (2013) 025009, http://dx.doi.org/10.1088/0965-0393/21/2/025009.
[22] Y. Zeng, A. Hunter, I.J. Beyerlein, M. Koslowski, A phase field dislocation dynamics model for a bicrystal interface system: An investigation into dislocation slip transmission across cube-on-cube interfaces, Int. J. Plast. 79 (2016) 293–313, http://dx.doi.org/10.1016/j.ijplas.2015.09.001.
[23] S. Xu, J.Y. Cheng, Z. Li, N.A. Mara, I.J. Beyerlein, Phase-field modeling of the interactions between an edge dislocation and an array of obstacles, Comput. Methods Appl. Mech. Engrg. 389 (2022) 114426, http://dx.doi.org/10.1016/j.cma.2021.114426.
[24] J.D. Eshelby, The determination of the elastic field of an ellipsoidal inclusion, and related problems, Proc. R. Soc. Lond. Ser. A Math. Phys. Eng. Sci. 241 (1226) (1957) 376–396, http://dx.doi.org/10.1098/rspa.1957.0133.
[25] Y.U. Wang, Y.M. Jin, A.G. Khachaturyan, Phase field microelasticity modeling of dislocation dynamics near free surface and in heteroepitaxial thin films, Acta Mater. 51 (14) (2003) 4209–4223, http://dx.doi.org/10.1016/S1359-6454(03)00238-6.
[26] M. Koslowski, M. Ortiz, A multi-phase field model of planar dislocation networks, Modelling Simul. Mater. Sci. Eng. 12 (6) (2004) 1087–1097, http://dx.doi.org/10.1088/0965-0393/12/6/003.
[27] D.W. Lee, H. Kim, A. Strachan, M. Koslowski, Effect of core energy on mobility in a continuum dislocation model, Phys. Rev. B 83 (10) (2011) 104101, http://dx.doi.org/10.1103/PhysRevB.83.104101.
[28] A. Hunter, I.J. Beyerlein, T.C. Germann, M. Koslowski, Influence of the stacking fault energy surface on partial dislocations in fcc metals with a three-dimensional phase field dislocations dynamics model, Phys. Rev. B 84 (14) (2011) 144108, http://dx.doi.org/10.1103/PhysRevB.84.144108.
[29] A. Hunter, R.F. Zhang, I.J. Beyerlein, The core structure of dislocations and their relationship to the material γ-surface, J. Appl. Phys. 115 (13) (2014) 134314, http://dx.doi.org/10.1063/1.4870462.
[30] Y. Su, S. Xu, I.J. Beyerlein, Density functional theory calculations of generalized stacking fault energy surfaces for eight face-centered cubic transition metals, J. Appl. Phys. 126 (10) (2019) 105112, http://dx.doi.org/10.1063/1.5115282.
[31] X. Wang, S. Xu, W.-R. Jian, X.-G. Li, Y. Su, I.J. Beyerlein, Generalized stacking fault energies and Peierls stresses in refractory body-centered cubic metals from machine learning-based interatomic potentials, Comput. Mater. Sci. 192 (2021) 110364, http://dx.doi.org/10.1016/j.commatsci.2021.110364.

[32] X. Peng, N. Mathew, I.J. Beyerlein, K. Dayal, A. Hunter, A 3D phase field dislocation dynamics model for body-centered cubic crystals, Comput. Mater. Sci. 171 (2020) 109217, http://dx.doi.org/10.1016/j.commatsci.2019.109217.
[33] L.T.W. Smith, Y. Su, S. Xu, A. Hunter, I.J. Beyerlein, The effect of local chemical ordering on Frank-Read source activation in a refractory multi-principal element alloy, Int. J. Plast. 140 (2020) 102850, http://dx.doi.org/10.1016/j.ijplas.2020.102850.
[34] L.T.W. Fey, S. Xu, Y. Su, A. Hunter, I.J. Beyerlein, Transitions in the morphology and critical stresses of gliding dislocations in multiprincipal element alloys, Phys. Rev. Mater. 6 (1) (2022) 013605, http://dx.doi.org/10.1103/PhysRevMaterials.6.013605.
[35] S. Xu, Y. Su, L.T.W. Smith, I.J. Beyerlein, Frank-Read source operation in six body-centered cubic refractory metals, J. Mech. Phys. Solids 141 (2020) 104017, http://dx.doi.org/10.1016/j.jmps.2020.104017.
[36] K. Kang, V.V. Bulatov, W. Cai, Singular orientations and faceted motion of dislocations in body-centered cubic crystals, Proc. Natl. Acad. Sci. USA 109 (38) (2012) 15174–15178, http://dx.doi.org/10.1073/pnas.1206079109.
[37] B. Yin, Z. Wu, W.A. Curtin, Comprehensive first-principles study of stable stacking faults in hcp metals, Acta Mater. 123 (2017) 223–234, http://dx.doi.org/10.1016/j.actamat.2016.10.042.
[38] C. Albrecht, A. Hunter, A. Kumar, I.J. Beyerlein, A phase field model for dislocations in hexagonal close packed crystals, J. Mech. Phys. Solids 137 (2020) 103823, http://dx.doi.org/10.1016/j.jmps.2019.103823.
[39] P.M. Kelly, H.P. Ren, D. Qiu, M.X. Zhang, Identifying close-packed planes in complex crystal structures, Acta Mater. 58 (8) (2010) 3091–3095, http://dx.doi.org/10.1016/j.actamat.2010.01.046.
[40] D. Rodney, L. Ventelon, E. Clouet, L. Pizzagalli, F. Willaime, Ab initio modeling of dislocation core properties in metals and semiconductors, Acta Mater. 124 (2017) 633–659, http://dx.doi.org/10.1016/j.actamat.2016.09.049.
[41] S. Xu, E. Hwang, W.-R. Jian, Y. Su, I.J. Beyerlein, Atomistic calculations of the generalized stacking fault energies in two refractory multi-principal element alloys, Intermetallics 124 (2020) 106844, http://dx.doi.org/10.1016/j.intermet.2020.106844.
[42] Y. Zeng, X. Cai, M. Koslowski, Effects of the stacking fault energy fluctuations on the strengthening of alloys, Acta Mater. 164 (2019) 1–11, http://dx.doi.org/10.1016/j.actamat.2018.09.066.
[43] Y. Su, S. Xu, I.J. Beyerlein, *Ab initio*-informed phase-field modeling of dislocation core structures in equal-molar CoNiRu multi-principal element alloys, Modelling Simul. Mater. Sci. Eng. 27 (8) (2019) 084001, http://dx.doi.org/10.1088/1361-651X/ab3b62.
[44] P.C. Vilalta, S. Sheikholeslami, K. Saleme Ruiz, X. C. Yee, M. Koslowski, Machine learning for predicting the critical yield stress of high entropy alloys, J. Eng. Mater. Tech. 143 (2) (2020) http://dx.doi.org/10.1115/1.4048873.
[45] J.R. Mianroodi, A. Hunter, I.J. Beyerlein, B. Svendsen, Theoretical and computational comparison of models for dislocation dissociation and stacking fault/core formation in fcc crystals, J. Mech. Phys. Solids 95 (2016) 719–741, http://dx.doi.org/10.1016/j.jmps.2016.04.029.
[46] L. Cao, A. Hunter, I.J. Beyerlein, M. Koslowski, The role of partial mediated slip during quasi-static deformation of 3D nanocrystalline metals, J. Mech. Phys. Solids 78 (2015) 415–426, http://dx.doi.org/10.1016/j.jmps.2015.02.019.
[47] A. Ruffini, Y. Le Bouar, A. Finel, Three-dimensional phase-field model of dislocations for a heterogeneous face-centered cubic crystal, J. Mech. Phys. Solids 105 (2017) 95–115, http://dx.doi.org/10.1016/j.jmps.2017.04.008.
[48] F. Bormann, R.H.J. Peerlings, M.G.D. Geers, B. Svendsen, A computational approach towards modelling dislocation transmission across phase boundaries, Phil. Mag. 99 (17) (2019) 2126–2151, http://dx.doi.org/10.1080/14786435.2019.1612961.
[49] A. Hunter, I.J. Beyerlein, Predictions of an alternative pathway for grain-boundary driven twinning, Appl. Phys. Lett. 104 (23) (2014) 233112, http://dx.doi.org/10.1063/1.4883396.
[50] A. Hunter, I.J. Beyerlein, Relationship between monolayer stacking faults and twins in nanocrystals, Acta Mater. 88 (2015) 207–217, http://dx.doi.org/10.1016/j.actamat.2014.12.045.
[51] X. Peng, A. Hunter, I.J. Beyerlein, R.A. Lebensohn, K. Dayal, E. Martinez, Non-orthogonal computational grids for studying dislocation motion in phase field approaches, Comput. Mater. Sci. 200 (2021) 110834, http://dx.doi.org/10.1016/j.commatsci.2021.110834.
[52] L.T.W. Fey, A. Hunter, I.J. Beyerlein, Phase-field dislocation modeling of cross-slip, J. Mater. Sci. 57 (2022) 1–15, http://dx.doi.org/10.1007/s10853-021-06716-1.
[53] A. Hunter, F. Saied, C. Le, M. Koslowski, Large-scale 3D phase field dislocation dynamics simulations on high-performance architectures, Int. J. High Perform. Comput. Appl. 25 (2) (2011) 223–235, http://dx.doi.org/10.1177/1094342010382534.
[54] A. Eghtesad, K. Germaschewski, I.J. Beyerlein, A. Hunter, M. Knezevic, Graphics processing unit accelerated phase field dislocation dynamics: Application to bi-metallic interfaces, Adv. Eng. Softw. 115 (2018) 248–267, http://dx.doi.org/10.1016/j.advengsoft.2017.09.010.
[55] A. Zhu, C. Jin, D. Zhao, Y. Xiang, J. Huang, A numerical scheme for generalized Peierls-Nabarro model of dislocations based on the fast multipole method and iterative grid redistribution, Commun. Comput. Phys. 18 (5) (2015) 1282–1312, http://dx.doi.org/10.4208/cicp.130114.270315a.
[56] A.F. Ware, Fast approximate Fourier transforms for irregularly spaced data, SIAM Rev. 40 (4) (1998) 838–856, http://dx.doi.org/10.1137/S003614459731533X.
[57] B. Liu, D. Raabe, F. Roters, P. Eisenlohr, R.A. Lebensohn, Comparison of finite element and fast Fourier transform crystal plasticity solvers for texture prediction, Modelling Simul. Mater. Sci. Eng. 18 (8) (2010) 085005, http://dx.doi.org/10.1088/0965-0393/18/8/085005.
[58] S. Zheng, D. Zheng, Y. Ni, L. He, Improved phase field model of dislocation intersections, npj Comput. Mater. 4 (2018) 20, http://dx.doi.org/10.1038/s41524-018-0075-x.
[59] S.Y. Hu, Y.L. Li, Y.X. Zheng, L.Q. Chen, Effect of solutes on dislocation motion — a phase-field simulation, Int. J. Plast. 20 (3) (2004) 403–425, http://dx.doi.org/10.1016/S0749-6419(03)00094-9.
[60] J.R. Mianroodi, P. Shanthraj, P. Kontis, J. Cormier, B. Gault, B. Svendsen, D. Raabe, Atomistic phase field chemomechanical modeling of dislocation-solute-precipitate interaction in Ni-Al-Co, Acta Mater. 175 (2019) 250–261, http://dx.doi.org/10.1016/j.actamat.2019.06.008.
[61] Z. Zheng, J. Chen, Y. Zhu, L. Zhao, M. Huang, S. Liang, Z. Li, An atomistically-informed phase-field model for quantifying the effect of hydrogen on the evolution of dislocations in FCC metals, Int. J. Plast. 138 (2021) 102937, http://dx.doi.org/10.1016/j.ijplas.2021.102937.
[62] M.L. Falk, J.S. Langer, Dynamics of viscoplastic deformation in amorphous solids, Phys. Rev. E 57 (6) (1998) 7192–7205, http://dx.doi.org/10.1103/PhysRevE.57.7192.
[63] N. Deka, R.B. Sills, Monte Carlo-discrete dislocation dynamics: a technique for studying the formation and evolution of dislocation structures, Modelling Simul. Mater. Sci. Eng. 30 (2) (2021) 024002, http://dx.doi.org/10.1088/1361-651X/ac41a2.
[64] T. Gerasimov, U. Römer, J. Vondřejc, H.G. Matthies, L. De Lorenzis, Stochastic phase-field modeling of brittle fracture: Computing multiple crack patterns and their probabilities, Comput. Methods Appl. Mech. Engrg. 372 (2020) 113353, http://dx.doi.org/10.1016/j.cma.2020.113353.